EXPERIMENTAL VERIFICATION OF THE INERTIAL OSCILLATIONS OF A FLUID IN A CYLINDER DURING SPIN-UP

K. D. Aldridge

British Columbia University

Prepared for:

Ballistic Research Laboratories

November 1975

BRL CR 273

BRL

AD

CONTRACT REPORT NO. 273

EXPERIMENTAL VERIFICATION OF THE INERTIAL OSCILLATIONS OF A FLUID IN A CYLINDER DURING SPIN-UP

Prepared by

University of British Columbia
Department of Geophysics and Astronomy
Vancouver, B. C., Canada

November 1975

USA BALLISTIC RESEARCH LABORATORIES
ABERDEEN PROVING GROUND, MARYLAND

UNCLASSIFIED
SECURITY CLASSIFICATION OF THIS PAGE (When Date Entered)

REPORT DOCUMENTATION PAGE		READ INSTRUCTIONS BEFORE COMPLETING FORM
1. REPORT NUMBER CONTRACT REPORT NO. 273	2. GOVT ACCESSION NO.	3. RECIPIENT'S CATALOG NUMBER
4. TITLE (and Subtitle) EXPERIMENTAL VERIFICATION OF THE INERTIAL OSCILLATIONS OF A FLUID IN A CYLINDER DURING SPIN-UP		5. TYPE OF REPORT & PERIOD COVERED Final 6. PERFORMING ORG. REPORT NUMBER
7. AUTHOR(s) K. D. Aldridge		8. CONTRACT OR GRANT NUMBER(s) DAAD05-74-Q-5383
9. PERFORMING ORGANIZATION NAME AND ADDRESS University of British Columbia Department of Geophysics and Astronomy Vancouver, B.C., Canada		10. PROGRAM ELEMENT, PROJECT, TASK AREA & WORK UNIT NUMBERS RDT&E 1W161102AH43
11. CONTROLLING OFFICE NAME AND ADDRESS USA Ballistic Research Laboratories Aberdeen Proving Ground, MD 21005		12. REPORT DATE NOVEMBER 1975 13. NUMBER OF PAGES 47
14. MONITORING AGENCY NAME & ADDRESS (if different from Controlling Office) US Army Materiel Command 5001 Eisenhower Avenue Alexandria, VA 22333		15. SECURITY CLASS. (of this report) Unclassified 15a. DECLASSIFICATION/DOWNGRADING SCHEDULE

16. DISTRIBUTION STATEMENT (of this Report)

A roved for public release; distribution unlimited.

17. DISTRIBUTION STATEMENT (of the abstract entered in Block 20, if different from Report)

18. SUPPLEMENTARY NOTES

19. KEY WORDS (Continue on reverse side if necessary and identify by block number)

liquid-filled projectiles
spin-up
eigenfrequency

20. ABSTRACT (Continue on reverse side if necessary and identify by block number)

The dependence of inertial oscillation frequency on time since a cylindrical container began rotating from rest is established experimentally for several axially symmetric modes of oscillation. The oscillations were excited by including a sinusoidal perturbation in the rotation speed of the container which served to establish an exchange of fluid between the viscous boundary layers and the interior. The interior is set into oscillation by the boundary layer flow and the resulting axial pressure differences are used to establish the amplitude

DD FORM 1 JAN 73 1473 EDITION OF 1 NOV 65 IS OBSOLETE

UNCLASSIFIED
SECURITY CLASSIFICATION OF THIS PAGE (When Date Entered)

20. of the inertial oscillation. The best agreement between our experiments and the theoretical work by Lynn (1973) on the time-dependence of inertial oscillation frequency occurs for the lowest frequency modes. From a limited study on amplitude of the inertial oscillations it appears that the growth rate of these disturbances is such that e^{-1} of the ultimate amplitude is achieved after one and a half spin up times from the time that the container is switched on. No non-linear effects in perturbation amplitude for the dependence of inertial oscillation frequency on time were found for the perturbation amplitudes used in these experiments.

Destroy this report when it is no longer needed.
Do not return it to the originator.

Secondary distribution of this report by originating or sponsoring activity is prohibited.

Additional copies of this report may be obtained from the National Technical Information Service, U.S. Department of Commerce, Springfield, Virginia 22151.

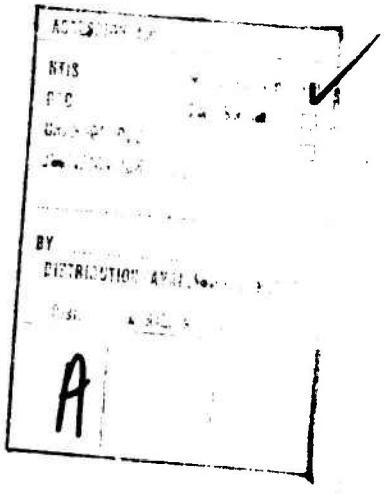

The findings in this report are not to be construed as an official Department of the Army position, unless so designated by other authorized documents.

The use of trade names or manufacturers' names in this report does not constitute indorsement of any commercial product.

TABLE OF CONTENTS

Notation and Range of Parameters used in the Experiments

	symbol	range of values	units
rotation speed	Ω	4-10	rad/sec
perturbation frequency	ω	6.308	rad/sec
perturbation half amplitude of container	ϵ	3-6.5	degrees
cylinder radius	a	9.53	cm
cylinder height	2c	19.01,38.02	cm
cylinder aspect ratio	$\alpha=\frac{2c}{a}$	1.99,3.98	
fluid density	ρ	0.9966-0.9976	gm/cm^3
kinematic viscosity	ν	.0086-.0095	cm^2/sec
sinusoidal disturbance pressure amplitude	Δp	1-3	mm water
time scale	$T = \frac{2c}{(\nu\Omega)^{\frac{1}{2}}}$	60-200	seconds
Ekman number	$E = \frac{\nu}{4\Omega c^2}$	8×10^{-7}-5×10^{-6}	

1. Introduction

The purpose of the experiments described in this report was to establish that axisymmetric inertial oscillations of a fluid in a cylindrical cavity could be excited by an axisymmetric perturbation of the container speed while the fluid was spinning up from rest. The success of these experiments would not only confirm the existence of inertial oscillations in a fluid during spin-up from rest but also that they could be excited by a time varying rotation speed of the container. Several axisymmetric modes of inertial oscillation have been excited in our experiments thus simultaneously confirming their existence and the method of excitation.

Prior to this experimental study only those oscillations of a rotating fluid which exist when the fluid is rotating as a solid body had been examined. The study of inertial oscillations under these conditions dates back to Kelvin (1880) who calculated the eigen frequencies for a cylinder of fluid in solid body rotation. Bjerknes and others (1933) revived the study of these oscillations in their work in the fields of oceanography and meteorology. More recently some experiments were carried out by Fultz (1959) who succeeded in exciting some axisymmetric oscillations in a rotating cylinder of fluid by forcing a small disc to oscillate on the axis of rotation at a frequency equal to a selected eigen frequency of the cylinder. The most recent work on inertial oscillations of a fluid in solid body rotation has been carried out by Aldridge and Toomre (1969) and Aldridge (1972, 1975). They excited axisymmetric inertial oscillations of a rotating fluid sphere by introducing a harmonic perturbation in the container rotation speed thus setting the fluid into oscillation by means of boundary layer pumping. The present study uses that method to excite inertial oscillations of the fluid in a cylinder during spin-up from rest.

Although the experiments described in this report are concerned with inertial oscillations they necessarily involved with the study of spin-up of the fluid in a cylinder from rest. Spin-up from rest is a strongly non linear process since the Rossby number is unity and it is only recently that this aspect of rotating fluids has been investigated in some detail. Experimental work by Watkins and Hussey (1973) and Weidman (1974) has extended the pioneering work of Wedemeyer (1964) in this field. We shall find it useful to refer to Wedemeyer's work because his model for spin-up from rest forms the basis of some recent analytical work by Lynn (1973) on inertial oscillations of liquid during spin-up from rest. Limitations of Wedemeyer's model discussed by Watkins and Hussey (1973) do not seriously concern us here because

our experiments appear to be within the limits established by these authors for the validity of the Wedemeyer model.

Fundamental to the Wedemeyer model, and in fact to all studies of spin-up, is the concept of the so-called spin-up time scale. Greenspan and Howard (1963) established the details for the process of linear spin-up a term which is associated with small changes in the rotation speed of the container from an initial value. Unless the body of fluid is very long compared to its diameter the most important dynamical process in the adjustment in the fluid speed to the new container speed is the advection of high angular momentum fluid towards the axis of rotation. This fluid replaces the fluid drawn into the boundary layers near the end walls of the container. It has been shown that the important time scale for the spin-up process - the so called spin-up time - is $L/(\nu\Omega)^{\frac{1}{2}}$ where L is a typical length parallel to the rotation axis, ν is the kinematic viscosity and Ω is the rotation speed of the fluid. For the case of linear spin-up the length L is half the cylinder height since this is the typical distance a fluid parcel must travel in the spin-up process. In the case of spin-up from rest authors have chosen to use the <u>total</u> height of the cylinder for this length scale. Although this does not seem justified in view of the above remarks we point out that the fluid changes its rotation speed from zero to Ω during spin-up from rest the larger length scale can be taken to reflect some average value in Ω for the fluid during the spin-up process.

The spin-up time scale is the geometric mean of two other time scales appropriate to the spin-up process. The short time taken to establish the boundary layers is $1/\Omega$ while the long time taken for small irregularities in the fluid rotation to diffuse is L^2/ν, the so-called diffusion time. In the work described here we scale all of our measured times with the spin-up time scale $L/(\nu\Omega)^{\frac{1}{2}}$ where L is the total height of the cylinder.

2. Experimental procedure

A cylindrical container, completely filled with water, is set into rotation at time $t=0$ about its axis of symmetry which is vertical. Superimposed on this rotation is a sinusoidal perturbation which continues all the while the cylinder is rotating. Thus the rotation of the container is specified as follows:

$$\Omega(t) = 0 \qquad t<0$$

$$\Omega(t) = \Omega + \varepsilon\omega \cos\omega t \qquad t\geq 0$$

The amplitude of the perturbation, $\varepsilon\omega$, is specified by the half angular displacement, ε, and the perturbation frequency, ω, while the mean rotation speed of the container is Ω. If the ratio of the perturbation frequency to the mean rotation speed ω/Ω coincides with one of the inertial oscillation frequencies of the cylinder then every particle will oscillate along a path determined by the eigenfunction for that particular frequency ratio ω/Ω. The response of the fluid to this perturbation was observed visually by releasing dye from thin wires stretched between the ends of the cylinder from points along a diameter of the cylinder. Quantitative measurement of the fluid response was obtained by monitoring disturbance pressure differences between two points on the axis of rotation. These pressure differences were measured with a differential type pressure transducer one port of which was connected by thick walled tubing to a hypodermic needle located on the axis of rotation. The other port and the filling hole at the top of the cylinder were open to the atmosphere.

The inertial oscillation frequency or eigenfrequency for a particular mode of oscillation depends not only on the geometry of the cylinder but also on the fraction of fluid which is spun up. Figure 1 illustrates schematically how this time dependence of eigenfrequency was established in the experiments. The vertical axis corresponds to the amplitude of the fluid response measured in terms of the dimensionless pressure coefficient $Cp = |\Delta p|/\rho\varepsilon\omega^2 a^2$ where Δp in the zero to peak sinusoidal (at frequency ω) disturbance pressure and ρ is the fluid density. The horizontal axis to the right is the adjustable frequency ratio Ω/ω of the container. We display the frequency ratio in this manner because in the experiments this ratio was selected by choosing a particular value of mean rotation speed Ω while the perturbation frequency ω was held fixed. The vertical bar in the $Cp - \Omega/\omega$ plane represents the inviscid response of a particular eigen oscillation at resonance. There are of course an infinite number of these modes and each one is broadened in reality by viscosity. Only one mode is shown here for clarity. The third axis corresponds to a measure of the time since the container was switched on, scaled in terms of the spin-up time $T = 2c/(\nu\Omega)^{1/2}$ where $2c$ is the cylinder height. We choose the exponential function of this time variable because this form is characteristic of the spin-up process

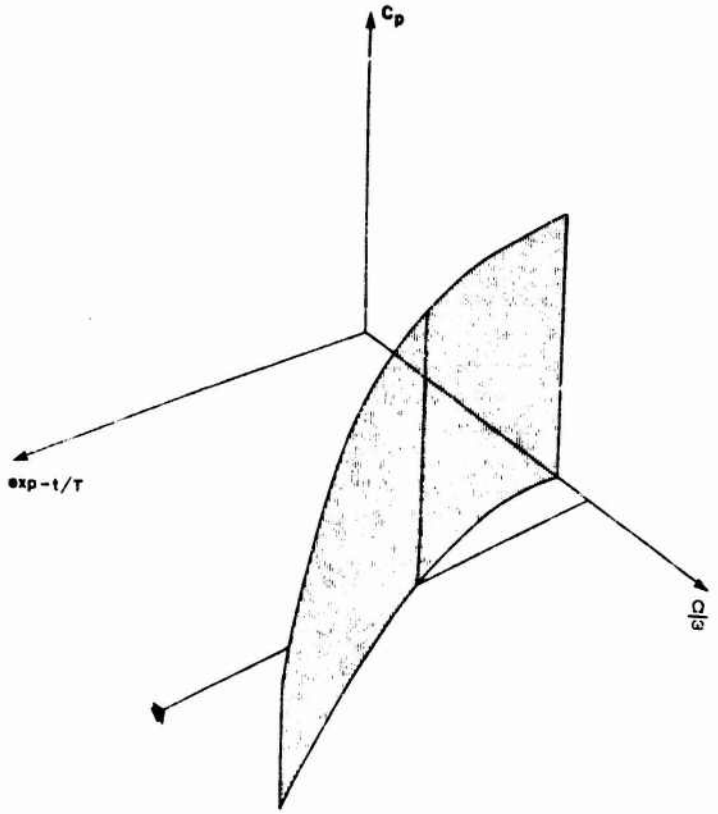

Figure 1. Schematic showing inviscid disturbance pressure response for spin-up from rest. Disturbance pressure coefficient, Cp , has a resonant amplitude for various values of frequency ratio $\frac{\Omega}{\omega}$ at time t since spin-up was begun. Time is scaled in terms of the spin-up time, T .

as used in the Wedemeyer model and Lynn's analysis. When $e^{-t/T} = 0$ the fluid rotates as a solid body except for the perturbation. Thus the $Cp - \Omega/\omega$ plane corresponds to the ultimate state of the fluid rotation. Values of $e^{-t/T}$ between one and zero correspond to the transient period which is of central interest in our experiments. The curve in the $e^{-t/T} - \Omega/\omega$ plane of figure 1 represents the change in eigenfrequency with time while the fluid is spinning up from rest. This curve is a schematic for the calculations of Lynn for the change in eigenfrequency with time. It is the purpose of our experiments to measure this time dependence and compare the experimental observations with Lynn's calculations.

Also shown in figure 1 is a schematic of the amplitude change of disturbance pressure with time as depicted by the vertical bars extending from the trace of the eigenfrequency-time curve in the $e^{-t/T} - \Omega/\omega$ plane. In the case of a real fluid some viscous broadening in frequency would exist for all time. No predictions for the change in response amplitude with time are included in Lynn's work.

A typical experimental run is shown by the line parallel to the $e^{-t/T}$ axis. Since Ω/ω was fixed for each run, we can associate the run with a point moving from left to right along this line with the passage of time since the container was switched on. When this point intersects the curve of eigenfrequency Ω/ω with time expressed as $e^{-t/T}$, a maximum in the sinusoidal disturbance pressure will be observed. If the fluid were inviscid no response would be observed until this point of intersection was reached. In fact the finite viscosity of the fluid produces a build up of the pressure before this point as well as a decay afterwards to a level appropriate to the ultimate disturbance pressure response. As mentioned earlier the finite viscosity also broadens the steady state response so that rather than depicting this response by a vertical line as shown in the $Cp - \Omega/\omega$ plane we should show a reduction in amplitude (Cp) with Ω/ω values on both sides of the vertical line.

The change in eigenfrequency Ω/ω with time during the spin-up period is found by measuring the time from the point at which the container is switched on to the peak disturbance pressure response for each of several values of Ω/ω for the container. This measurement of time is made from a chart record of the disturbance pressure for the entire period from container switch-on until the peak disturbance pressure is obtained. For values of Ω/ω for the container speed only slightly greater than Ω/ω for a particular eigen mode of the cylinder in the steady state ($t \to \infty$) both the time until maximum disturbance pressure is reached and the amplitude of the disturbance pressure will be greatest. The time from container switch-on until disturbance pressure maximum and the amplitude of this disturbance pressure difference both decrease with greater values of $\frac{\Omega}{\omega}$ (for the container) relative to the steady state value of Ω/ω for the mode

being studied. Ultimately disturbance pressure differences will become too small to detect when $\frac{\Omega}{\omega}$ for the container is very much greater than $\frac{\Omega}{\omega}$ for the mode being studied.

3. Theoretical background

The main purpose of this study is to compare our experimental results with predictions by Y. M. Lynn (1973) on the change in inertial oscillation frequencies with time for a cylinder of fluid during spin-up from rest. For completeness in this comparison we summarize some of the pertinent points of Lynn's analysis. In particular we are concerned with the assumptions inherent in Lynn's work since these will be important in any comparison between experiment and theory.

Spin-up of the fluid from rest is assumed to be given by a model due to Wedemeyer (1964). In this model boundary layers form at the container walls within a few revolutions after the container is set rotating. These layers are responsible for a secondary flow which removes non-rotating fluid from the interior in order to spin it up. This spun-up fluid is subsequently returned to the interior. Fluid which has been spun-up is convected across the interior until the fluid which had been at rest is completely removed and replaced. An analytical description of this process begins by assuming that the fluid can be divided into two regions, a boundary layer in which viscous effects are important and an essentially inviscid interior. The velocity field in the interior consists of a primary circulation and a secondary circulation which is $O(E^{\frac{1}{2}})$ where

$$E = \frac{\nu}{4\Omega c^2}$$

is the Ekman number. At this point we note that it follows from the equations of motion that to this order the velocity field is independent of the direction parallel to the axis of rotation. This statement is confirmed by experimental observations by Greenspan (1968) and others. It is in effect a statement of the Proudman-Taylor theorem which says that for slow, steady, inviscid adjustments of the velocity field, both the velocity and pressure are independent of height to all orders.

Some important assumptions must now be made in order to proceed analytically. It is necessary to obtain a relationship between the primary azimuthal velocity and the secondary radial velocity in the inviscid interior. This relationship is obtained from boundary layer analysis. Wedemeyer assumed that the boundary layer velocity field is steady, an assumption which does seem to be valid for small Rossby numbers. The validity of this assumption for Rossby numbers of order

unity as in the case of spin-up from rest will limit the validity of the Wedemeyer model.

If we call u_1 the secondary interior radial velocity and v_o the primary interior azimuthal velocity the relationship between these two velocities is found by Wedemeyer to be

$$u_1 = -\chi E^{\frac{1}{2}} (\Omega r - v_o)$$

where $\chi = 0.866$ is a constant. This form of the relationship was assumed by Wedemeyer by adopting a linear interpolation between the velocity $u_1 = -0.866 E^{\frac{1}{2}}\Omega r$ for the initial period after the container is turned on and the ultimate velocity $u_1 = 0$ when solid body rotation is achieved. Greenspan (1968) on the other hand obtains the same form as Wedemeyer but uses $\chi = 1.0$ based on an extrapolation from the case of linear spin-up for an arbitrary but axially symmetric container geometry. Rott and Lewellen (1966) use a value of $\chi = 1.1$. Various authors including Watkins and Hussey (1973) and Lynn (1973) have adopted Wedemeyer's method but have used $\chi = 1.0$ instead of $\chi = 0.866$. We shall consider the effect of choice for this constant in our discussion of the experimental results.

The primary azimuthal velocity field established from the above assumptions and used by Lynn as the unperturbed state for his analysis is:

$$\frac{v_o(r,t)}{\Omega} = \frac{r - \frac{f^2}{r}}{1 - f^2} \qquad f \leq r \leq 1$$

$$= 0 \qquad 0 \leq r \leq f$$

where $f = e^{-\chi E^{\frac{1}{2}} t}$ with $\chi = 1.0$.

This expression describes a cylindrical velocity front which moves radially inward from the sidewall across the cylinder. The cylinder is divided into two regions: the outer region has azimuthal velocity which depends on radius according to the above relationship while the inner region contains the central core which is at rest. Lynn shows that the position of the velocity front can be regarded as stationary for the period of the fluid oscillation which is $O(\frac{1}{\Omega})$ because this time is short compared to the time

scale $2c/(\Omega\nu)^{\frac{1}{2}}$ of movement of the front. Thus the quantity f which is the position of the velocity front is assumed constant in Lynn's perturbation analysis.

Inertial oscillations for a cylinder of fluid with the velocity field described above are found from a set of perturbation equations by looking for solutions of the form

$$\cos Kz \; e^{-i(\omega t - m\theta)}$$

where z and t are the vertical coordinate scaled by the cylinder height and the time scaled by the rotation period respectively. The number of waves in the azimuthal direction θ is given by m. The quantity $K = \frac{k\pi}{\alpha}$ where k is the number of waves in the direction parallel to the rotation axis and the aspect ratio α is the ratio of the cylinder height to radius.

For the case $E = 0$ (inviscid) and $m = 0$ (axially symmetric) Lynn obtains solutions for perturbation velocity and pressure in each of the two regions separated by the inward moving velocity front. Equality of the perturbation velocity and pressure in each of the two regions at this front leads to a set of homogeneous linear equations for the amplitudes of these disturbances. The existence of a solution to these equations gives a relationship involving the dependence of the inertial oscillation frequency on time since the container was switched on. This latter equation is solved numerically. Lynn's numerical results will be presented later when we compare them with the experimental results.

After several spin-up times since the container was switched on the time-dependent inertial oscillation frequencies should approach those found by Kelvin (1880) for a cylinder of fluid in solid body rotation. In this case

$$\left(\frac{\Omega}{\omega}\right)_{k,i} = \frac{1}{2}\left[\left(\frac{\gamma_i}{K}\right)^2 + 1\right]^{\frac{1}{2}} \qquad (1)$$

where γ_i is the i^{th} root of $J_1(x) = 0$. We use the (k,i) pair to denote the axisymmetric inertial oscillations: k is the number of waves or cells in the axial direction while i is the number of waves or cells in the radial direction. In our experiments k is always an even number because we excite only equatorially symmetric oscillations by our boundary layer pumping technique. Numerical values from the above relationship do agree with those from Lynn's analysis for $t \to \infty$.

We now summarize the assumptions used in obtaining the dependence of eigenfrequency on time since the container was switched on:

(i) the boundary layers are assumed to be steady in order to obtain the Wedemeyer velocity front solution required for spin-up,

(ii) the radially moving velocity front is assumed stationary in the calculation of the eigenfrequencies and

(iii) the fluid is assumed inviscid (E = 0) for the eigenfrequency calculations.

These assumptions will be discussed in our comparison of the analytically determined eigenfrequencies with those from experiment.

4. Experimental results

We begin by presenting the quantitative experimental results based on the disturbance pressure measurements described in section 2. Our first task was to establish to that the oscillations observed by disturbance pressure measurements are indeed the inertial oscillations we are seeking. Pressure differences between a point at the centre of the cylinder ($\alpha = 1.99$) and a point on the axis at the top of the cylinder were measured at selected values of the ratio $\frac{\Omega}{\omega}$, rotation speed divided by oscillation frequency, near an expected resonance value of this ratio. These measurements were carried out after the fluid had been spun up to the mean value of the rotation speed of the container, Ω. Displayed in figure 2 are the observed pressure differences expressed in terms of the dimensionless pressure coefficient $C_p = |\Delta p|/\rho\varepsilon\omega^2 a^2$ for each of several values near $\frac{\Omega}{\omega} = 0.7873$ which is the inertial oscillation (2,1) for an inviscid fluid with $k = 2$ and $i = 1$. Each of the points shown in the figure is an average of more than ten disturbance pressure measurements for a particular ratio $\frac{\Omega}{\omega}$. Clearly a resonance exists as shown by the maximum response near the predicted ratio $\frac{\Omega}{\omega} = 0.7873$. The amplitude of the container perturbation was $\varepsilon = 3.45°$. We show later that this amplitude is small enough to render non-linear effects associated with the perturbation negligible for our experiments.

Further evidence that we are indeed observing inertial oscillations in these experiments is provided by the corresponding disturbance pressure results near $\frac{\Omega}{\omega} = 1.220$ which is the (2,2) mode of oscillation in our notation. These results are shown in figure 3 for $\varepsilon = 3.35°$.

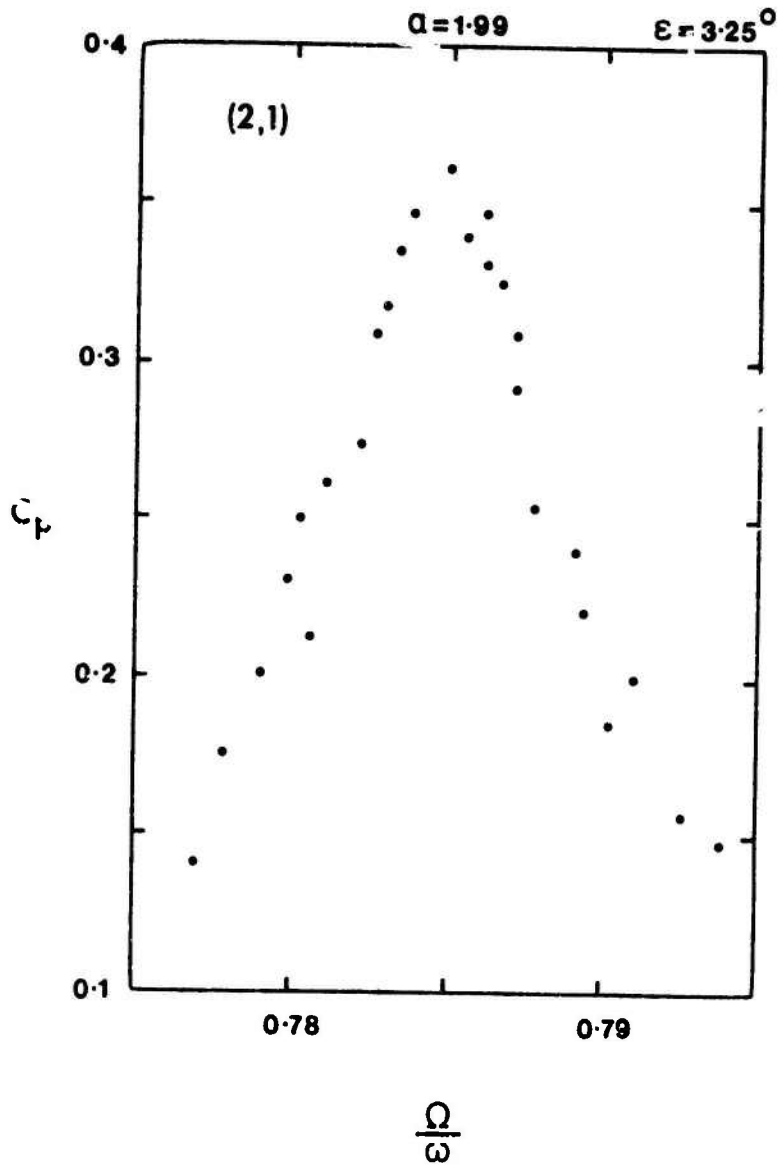

Figure 2. Disturbance pressure response ($t \to \infty$) for the (2,1) mode of the cylinder with aspect ratio α=1.99. Amplitude perturbation ε=3.25°.

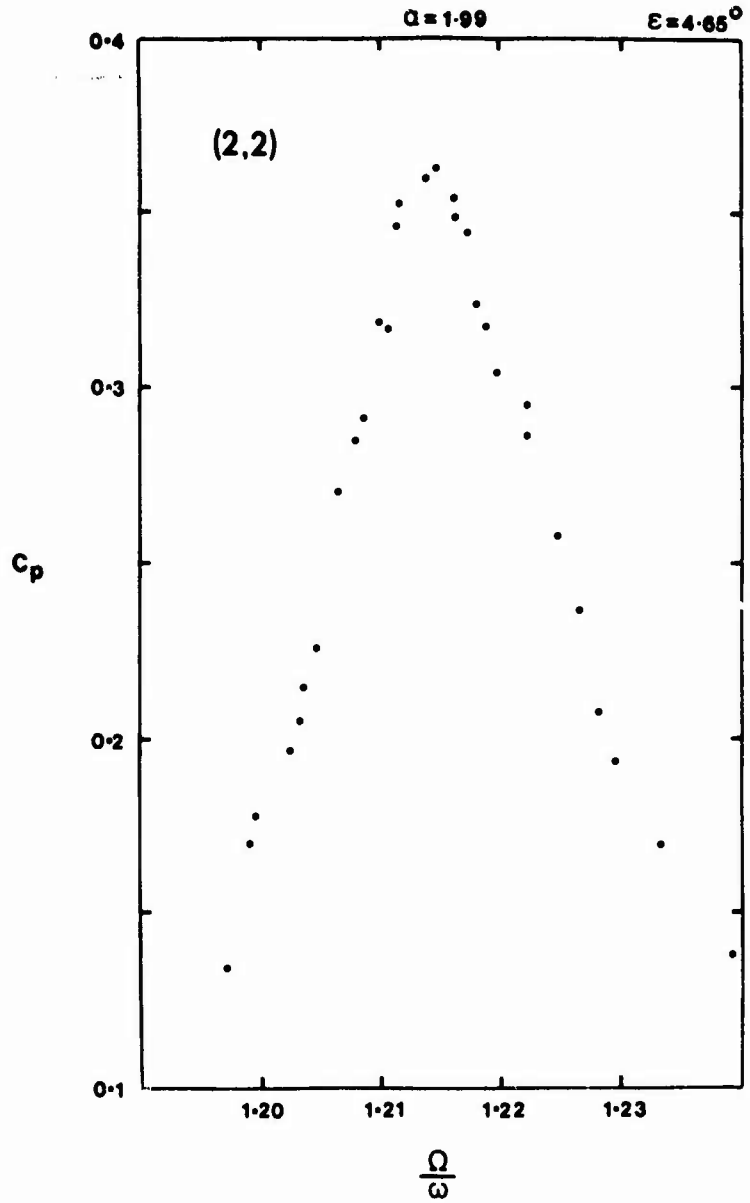

Figure 3. Disturbance pressure response ($t \to \infty$) for the (2,2) mode of the cylinder with aspect ratio α=1.99. Amplitude perturbation ε=4.65°.

We note that in figures 2 and 3 there is a small discrepancy between the observed and predicted frequency ratio $\frac{\Omega}{\omega}$ for the maximum value of C_p . The source of this error will be discussed in section 5. Our primary concern is that we have identified the observed pressure response with the inertial oscillations.

The dependence of inertial oscillation frequency on time while the fluid is spinning up from rest was found by the procedures outlined in section 2. As explained in that section the container is switched on at time $t = 0$ and rotates as $\Omega(t) = \Omega + \varepsilon\omega \cos\omega t$. Throughout the time that the fluid is being spun up disturbance pressure differences between two points on the rotation axis are recorded on chart paper. Displayed in figure 4 is a time history of the disturbance pressure for each of a series of values $\frac{\Omega}{\omega}$ near the (2,2) mode for a perturbation amplitude $\varepsilon = 5.46°$. Each trace corresponds to a path in the

$$e^{-t/T} - \Omega/\omega$$

plane shown by the line in figure 1 parallel to the $e^{-t/T}$ axis. The small arrow on the Ω/ω axis of figure 4 indicates the predicted value of $\frac{\Omega}{\omega} = 1.220$ for an inviscid fluid oscillating in the (2,2) mode, after the container has been rotating for a sufficiently long period that the fluid is spun-up.

For each run with $\frac{\Omega}{\omega} > 1.220$ a maximum in the disturbance pressure record is apparent, indicating that the (2,2) mode has been excited. For values of $\frac{\Omega}{\omega} > 1.220$ the maximum value in disturbance pressure with time occurs sooner for greater values of $\frac{\Omega}{\omega}$. Each of the traces has been truncated at about one spin-up time after peak disturbance pressure has been observed. Hence the locus of end points for the chart records sketches out the line of maxima in disturbance pressures. Following along this line we can see that the oscillation frequency ω , scaled with rotation speed, Ω , increases as time since the container was switched on increases. We shall see shortly that this behavicur is consistent with Lynn's analysis.

The measured disturbance pressures extend over several cycles of oscillation since the fluid has finite viscosity which results in frequency broadening of the resonance. This broadening in frequency is observed in the experimental runs because inertial oscillation frequency depends on the time since container switch on. In fact the change in the length of the disturbance pressure signals from one run to the next provides a qualitative measure of the time dependence of inertial oscillation frequency. Since the duration of the disturbance pressure signal gets longer for values of $\frac{\Omega}{\omega}$ near the predicted ($t \to \infty$) resonance $\frac{\Omega}{\omega} = 1.220$, we know that what might be called the disturbance pressure surface must have its maximum values along a line nearly parallel to the $e^{-t/T}$ axis. Hence for very long times since the container is switched on the experiments show that the inertial oscillation frequency is almost

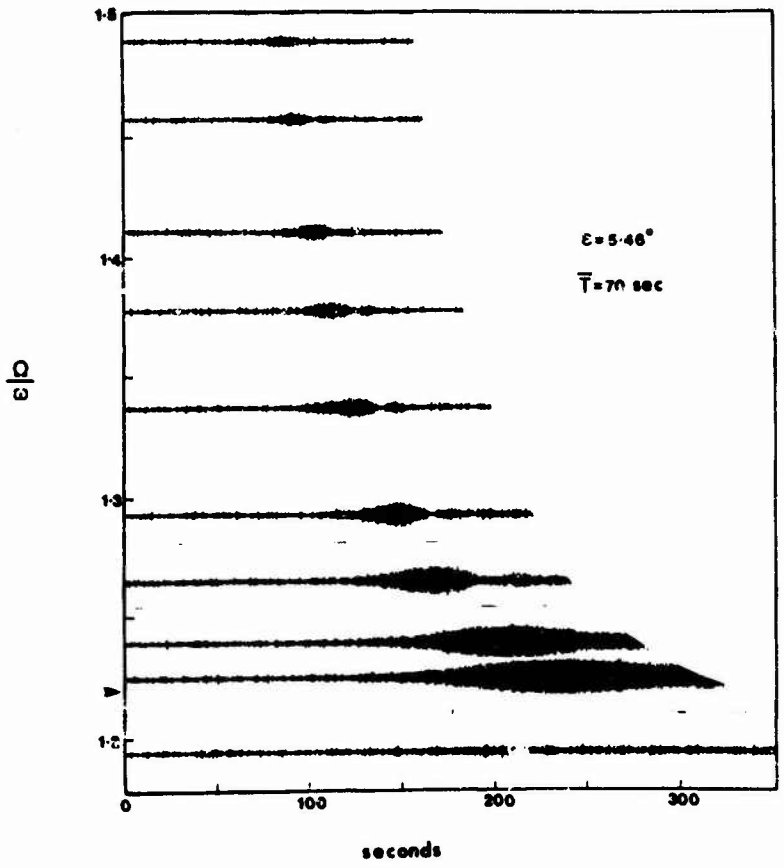

Figure 4. Time histories of disturbance pressue from container switch-on (t=0) for various values of rotation speed Ω scaled by oscillation frequency ω near the (2,2) mode. Amplitude perturbation $\varepsilon=5.46^{\circ}$; typical spin-up time scale $\bar{T}=70$ seconds.

independent of time. This too is consistent with Lynn's analysis.

For the run shown at the bottom of figure 4 for $\frac{\Omega}{\omega} < 1.220$ very little increase in disturbance pressure is observed over the background noise. This result is consistent with the above remarks on both the qualitative dependence of inertial oscillation frequency on time and the viscous broadening of the resonance peak. Had the value of $\frac{\Omega}{\omega}$ for this run been slightly larger but still less than 1.220 we would have expected a monotonic increase in disturbance pressure because we would be cutting the disturbance pressure surface on its convex flank rather than its concave flank as was the case for all the other runs with $\frac{\Omega}{\omega} > 1.220$. In fact a close inspection of figure 4 reveals a very small disturbance pressure signal with a monotonic increase over time since switch on. The small size of this pressure signal might at first seem surprising but reference to figure 3 shows that the bandwidth for the resonance is very narrow so that a rapid decrease in pressure response away from resonance is expected.

A quantitative measure of the dependence of inertial oscillation frequency on time since container switch-on is found from a direct measurement of time between switch-on and the peak response in disturbance pressure. Plotted in figure 5 for each of the runs shown in figure 4 are these times, scaled by the spin-up time scale

$$T = \frac{2c}{(\nu\Omega)^{\frac{1}{2}}}$$

and expressed in terms of $e^{-t/T}$. A typical value for the spin-up time in these experiments is $\overline{T} = 70$ seconds. For comparison with theory the dash-dot line in figure 5 is the calculated dependence of inertial oscillation frequency on time since the container was switched on. Agreement between experiment and theory is reasonable, although the tendency for the experiments to show a larger shift in frequency than the theory at a fixed time since container switch on is noteworthy since this effect will be found to a greater or lesser extent in all of the experiments. Expressed in the time domain this means that the experiments show the arrival in time of the (2,2) mode of oscillation to be later than predicted by Lynn's work. This statement follows obviously from figure 5 if we remember that real time runs from top to bottom of the figure for a given choice of $\frac{\Omega}{\omega}$.

Shown in figure 6 is the maximum disturbance pressure amplitude for each of the runs of figure 4 plotted against the time since container switch-on in the units $e^{-t/T}$. The growth of the (2,2) mode can be obtained directly from figure 6 to be that e^{-1} of the ultimate disturbance pressure difference is achieved after approximately 1½ spin up times since the apparatus is set rotating. Although this measurement of growth rate is an important one, it was not pursued in this set of experiments for two major reasons. First, since it was not possible

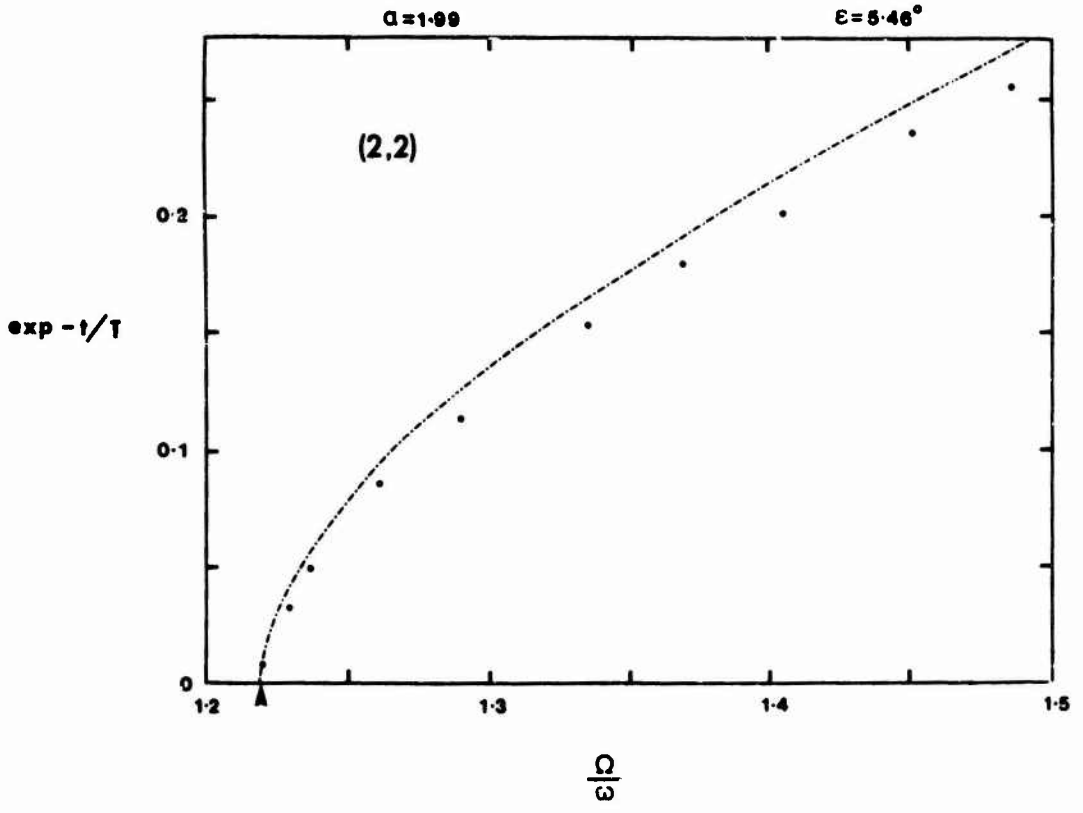

Figure 5. Time interval t from container switch-on until peak disturbance pressure from records of figure 4. Points show dependence of inertial oscillation frequency on time since switch-on for (2,2) mode in the cylinder α=1.99. The curve showing this same dependence is from Lynn (1973).

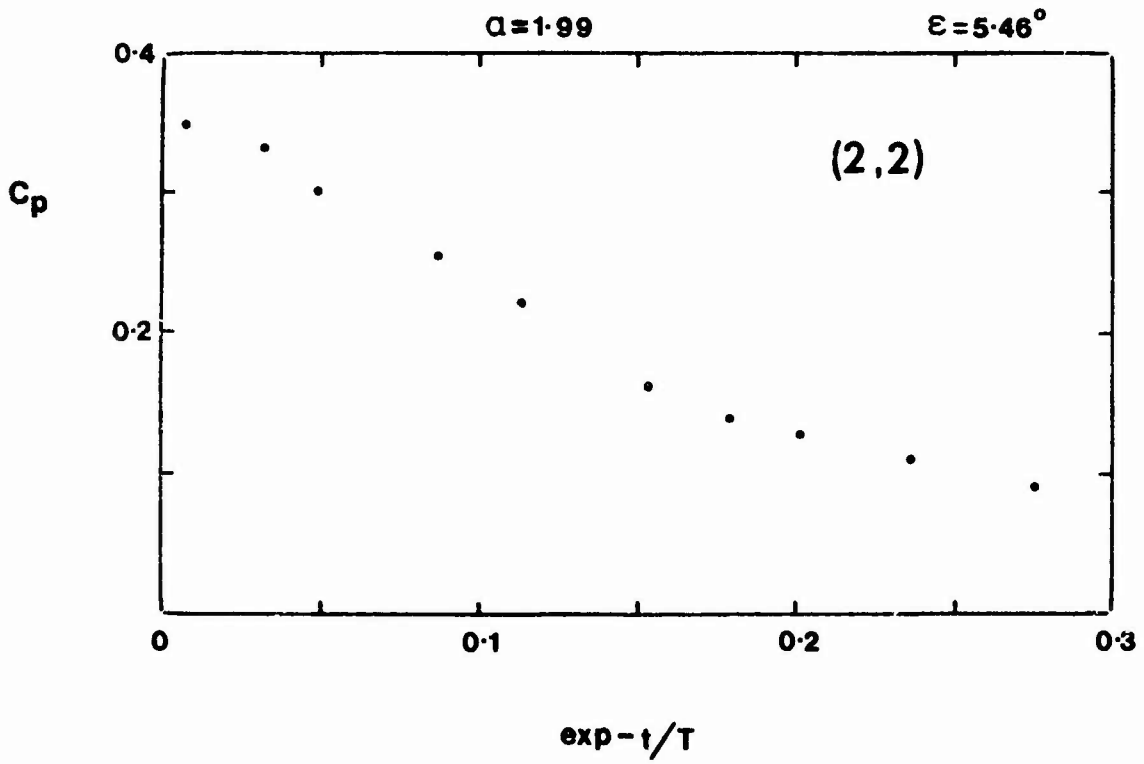

Figure 6. Disturbance pressure coefficient from data of figure 4 showing growth of inertial oscillation over time since switch-on. Note that real time increases from right to left.

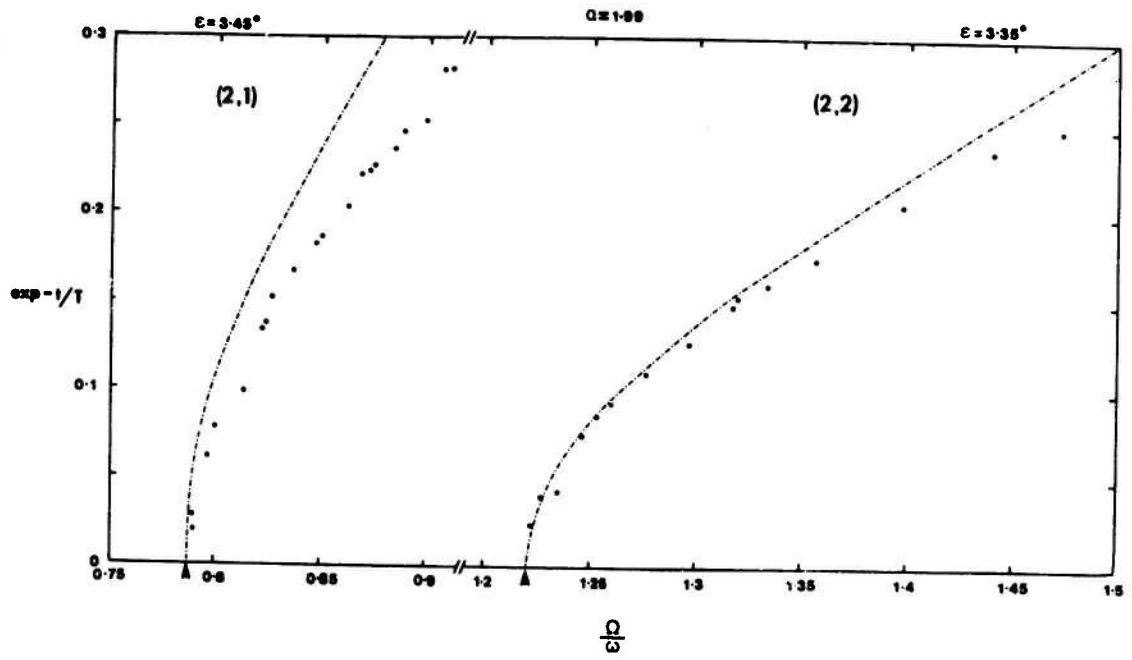

Figure 7. Points show dependence of inertial oscillation frequency on time since container switch-on for (2,1) mode (left)and (2,2) mode (right) in the cylinder α=1.99. Curves are from Lynn (1973).

to adjust the acceleration of the container over the switch-on period, no measurements could be carried out to determine the effect of container acceleration on amplitude build up of the inertial oscillation. In our apparatus the spin-up period of the container was fixed by the feedback control system, the torque capability of the drive motor and the moment of inertia of the rotating mass. Thus the switch-on was not perfectly impulsive as implied in section 1 but took approximately 3 oscillations (about 3 seconds) to achieve the quasi-steady state, $\Omega + \varepsilon\omega \cos\omega t$. This point is discussed further in our proposal to extend the experiments described in this report.

The second reason for not pursuing amplitude response was also a practical one. While our experiments were conducted with water as the working fluid our pressure transducer required an inert working fluid such as silicone oil. Small changes in surface tension at the oil-water interface due to impurities or for other reasons made consistent amplitude results difficult to achieve. The calibration of the pressure transducer, described in appendix I, provided a measure of the repeatability of the amplitude of our disturbance pressure measurements. Only the results shown in figure 6 were deemed acceptable for presentation because of the above limitations. We note however that small changes in the amplitude of the pressure response from one experimental run to another which might preclude using the disturbance pressure amplitudes themselves will still give reliable information on the dependence of inertial oscillation frequency on time since container switch-on.

The time from container switch-on until peak disturbance pressure for the (2,1) mode for $\varepsilon = 3.45°$ and again with $\alpha = 1.99$ is shown on the left side of figure 7. As in figure 5 for the (2,2) mode each point represents an experimental run for a fixed value of $\frac{\Omega}{\omega}$ near the expected resonance. Shown for comparison on the right side of figure 7 is a similar set of results for the (2,2) mode, again for the cylinder $\alpha = 1.99$ but at a smaller perturbation amplitude $\varepsilon = 3.35°$ than for runs presented in figure 5. Immediately obvious from figure 7 is the greater shift in frequency of the (2,2) mode relative to the (2,1) mode for a fixed time since switch-on. This difference between the (2,1) and (2,2) modes is even more pronounced in Lynn's analytical results shown by the dash-dot lines. Again the experiments indicate a greater shift in frequency than theory would predict and this discrepancy is even greater in the case for the (2,1) mode than for the (2,2) mode. A general statement which summarizes the results in figure 7 is that for a given axial structure ($k = 2$) agreement with theory is best for greater radial structure.

A further set of experimental runs were made with the same cylinder ($\alpha = 1.99$) to investigate the change in frequency with time since switch-on for the (4,2) mode. This mode was chosen since it has the same radial structure ($i = 2$) as the (2,2) mode but double the axial structure. In order to obtain a disturbance pressure response for the (4,2) mode it was necessary to raise the tip of the hypodermic needle, which served to communicate pressure changes to the transducer, to a point half way down to the centre of the cylinder from the top. This step is

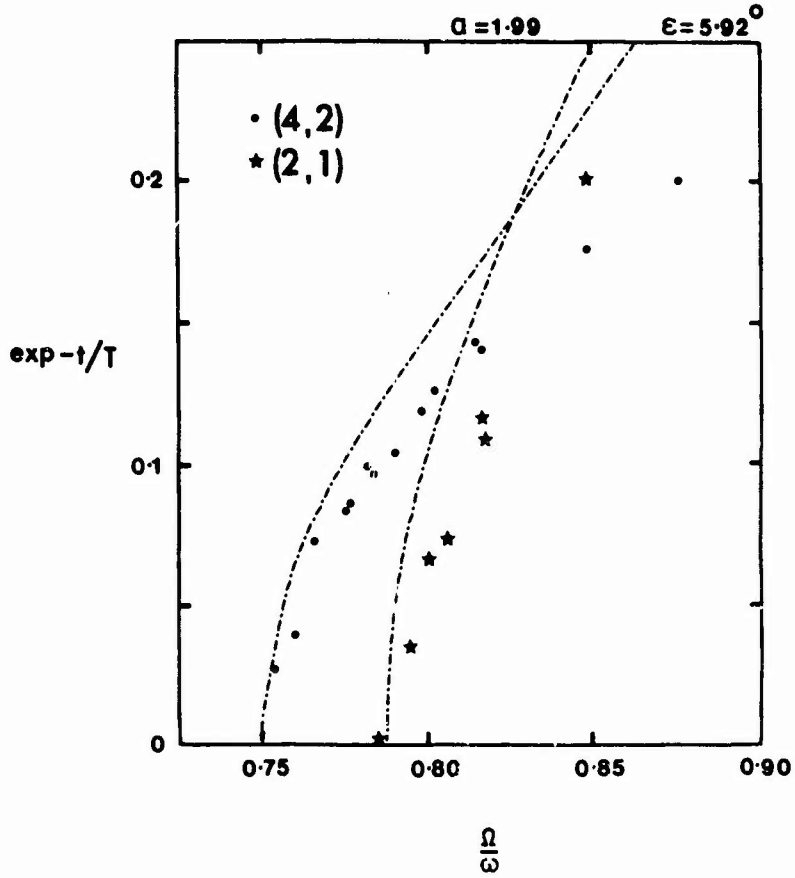

Figure 8. Dependence of inertial oscillation frequency on time since container switch-on for (4,2) mode (closed circles) and (2,1) mode (stars) in the cylinder α=1.99. Probe tip is half way between the top and centre of the cylinder. Amplitude perturbation ε=5.92°. Curves are from Lynn (1973).

obvious if we recall that since a mode with four cells in the axial direction will have opposing axial pressure gradients in each cell no net pressure difference will be observed when the measurement distance spans one pair of cells. We note also, however, that modes with only 2 cells in the axial direction will still be observed when the probe tip is raised to this new position but with only about half the amplitude as observed with the probe tip at the centre. Thus positioning the probe tip at the centre acts somewhat as a filter which discriminates against those modes with several cells in the axial direction and especially those modes having an even number of cells. This serves to explain in part why it is possible to make meaningful measurements on only a few modes of oscillation when in fact the spectrum of inertial oscillations everywhere dense. Also limiting the number of modes observed is our method of excitation itself since our perturbation of the container rotation speed will only be coupled well to a few of the spatially simple modes of oscillation.

Shown in figure 8 by the solid circles are the observed times t from container switch-on until peak disturbance pressure, again in terms of $e^{-t/T}$, for the (4,2) mode in the cylinder $\alpha = 1.99$. Due to the proximity of the (4,2) mode to the (2,1) both these modes could be observed on some chart records. The stars in figure 8 indicate the "arrival" of the (2,1) mode. Although the amplitude $\varepsilon = 5.92°$ was almost double that for the previous experiments involving the (2,1) mode (figure 7) the disturbance pressure response was less than ¼ of that expected even after taking into account the reduction due to the probe being raised. These difficulties led to a greater scatter in the results compared to previous experimental runs. The source of this reduction in amplitude is unknown.

The dash-dot lines shown in figure 8 are Lynn's calculated frequency shifts for the (4,2) and (2,1) modes. We note that experimental results for the (4,2) mode fall below the line predicted but to a greater extent than in the case of the (2,2) mode (figure 7). Hence decreasing the axial structure, keeping the radial structure constant results in better agreement with theory.

The experimental results presented in figures 7 and 8 can be summarized after the introduction of some terminology needed to describe the inertial oscillations. Recalling that a mode of inertial oscillation is specified by the (k,i) index, we can describe the spatial structure of the velocity stream function in terms of bounding nodal surfaces which will be rectangles in a plane containing the axis of rotation. The smallest rectangle without any interior nodal surfaces has been termed a cell. Such a cell has the ratio of its axial to radial dimensions of order $\frac{\alpha i}{k}$. Each mode of inertial oscillation has 2ki cells. Of the three modes (2,1), (2,2) and (4,2)studied in figures 7 and 8, the (2,2) mode, which most closely agrees with theory in its frequency dependence on time since switch-on, has cells with the largest ratio of axial to radial dimensions.

Modes of oscillation which have relatively long (axial) and narrow (radial) cells occur at low frequencies, ω , relative to the rotation speed. This statement follows directly from relation (1) given in section 3 since

$$\alpha \frac{\gamma i}{k\pi}$$

is also a measure of the axial to radial dimensions of a cell. Physically low frequency modes mean that most of the fluid movement is parallel to the axis of rotation as we would expect since the individual cells are tall and narrow. If we recall that the restoring force of inertial oscillations arises from the rotation, the lowest frequency modes are the ones which "feel" the rotation least. Hence from the experiments we have described so far it appears that Lynn's analysis has its best application for low frequency oscillations which have their motion predominantly parallel to the axis of rotation.

Reference to relation (1) reveals that a further investigation of the above remarks on Lynn's analysis could be carried out by adjusting the cylinder aspect ratio, α . The relation (1) tells us that the height of the cell should be measured not simply by k but by $K = \frac{k\pi}{\alpha}$ since in fact this is what determines the physical height of the cell relative to its radial extent or width.

For a cylinder $\alpha = 3.98$, twice the height of the previous cylinder, a series of experiments on the (2,1) mode, previously presented in figure 7, were carried out. The dependence of frequency on time since container switch on for the (2,1) mode is shown in figure 9. We note first that the frequency ratio $\frac{\Omega}{\omega}$ for $t \to \infty$ is of course larger than in the case for $\alpha = 1.99$ because the particle motion is more predominantly parallel to the rotation axis the cylinder being taller, even though there are still 2 cells in the axial and 1 in the radial direction.

Agreement between the experiments and theory shown by the dash-dot line from Lynn's work is much better than in the case of figure 7 for $\alpha = 1.99$. This improvement in agreement with theory is just as anticipated on the basis of our earlier generalizations.

The study of the (4,2) mode in the cylinder $\alpha = 1.99$ (figure 8) was repeated for the cylinder $\alpha = 3.98$. Shown in figure 10 by the solid circles is the observed shift in frequency of the (4,2) mode as measured by the time until maximum disturbance pressure difference from container switch-on. As in the previous experiment for the (2,1) mode (figure 9) the value of $\frac{\Omega}{\omega}$ for $t \to \infty$ is greater for the container $\alpha = 3.98$ than for $\alpha = 1.99$ as would be expected from

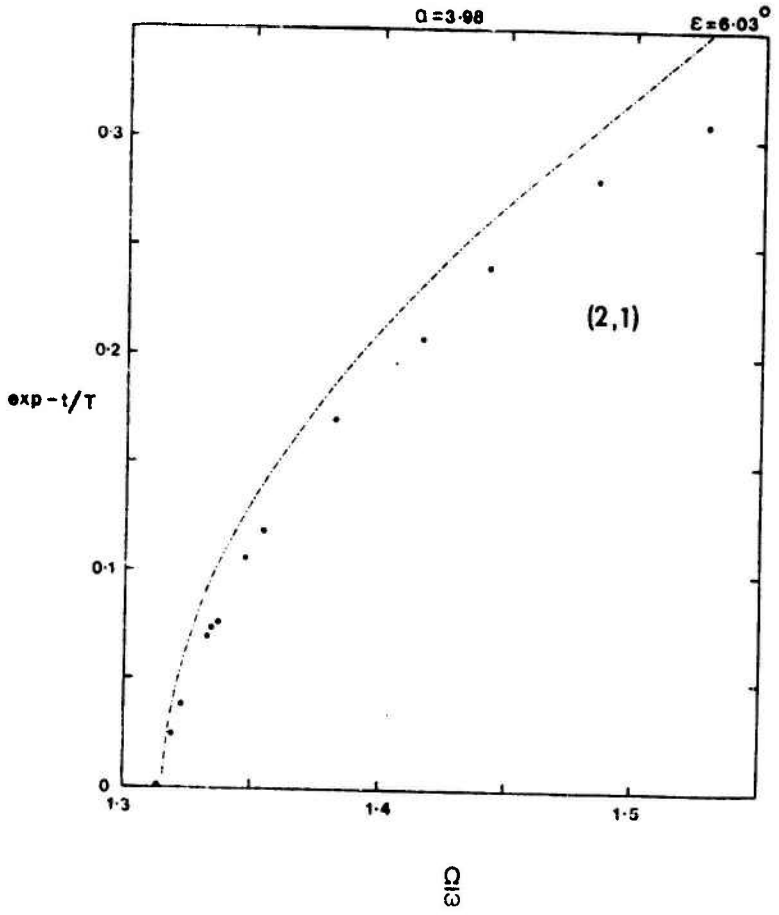

Figure 9. Dependence of inertial oscillation frequency on time since container switch-on for (2,1) mode in the cylinder α=3.98. Amplitude perturbation ε=6.03°. Curve is from Lynn (1973).

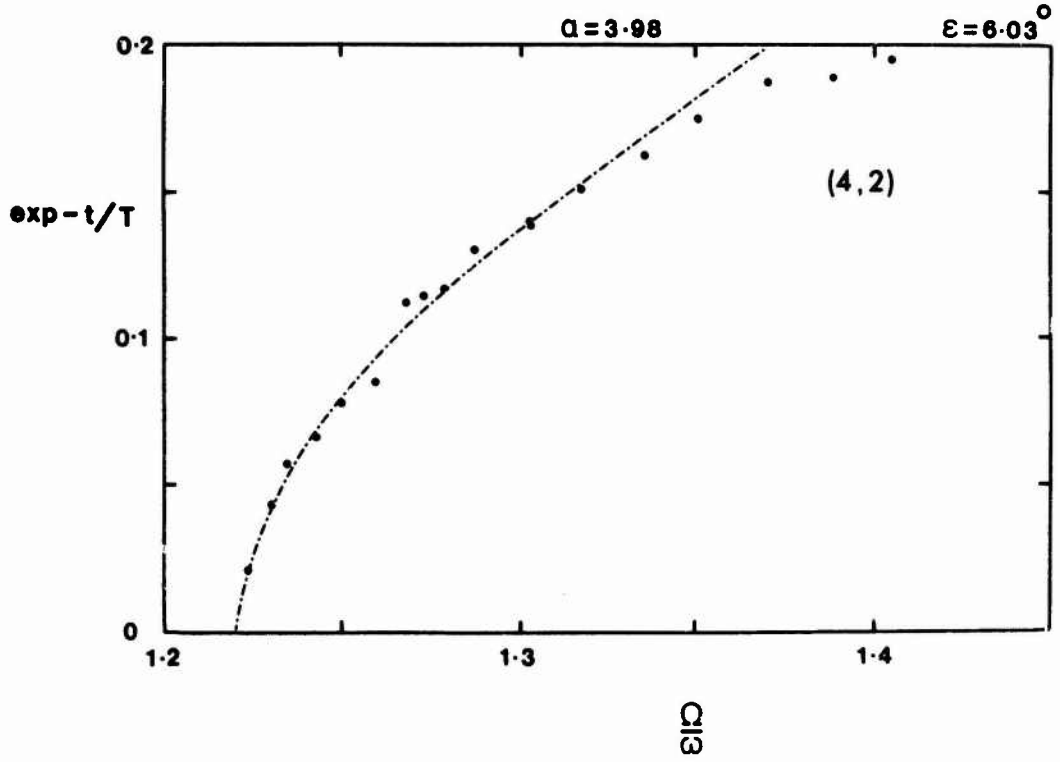

Figure 10. Dependence of inertial oscillation frequency on time since container switch-on for (4,2) mode in the cylinder α=3.98. Probe tip is half way between the top and centre of the cylinder. Amplitude perturbation ε=6.03°. Curve is from Lynn (1973).

relation (1). Hence the oscillation frequency ω is smaller relative to Ω and we would anticipate better agreement with theory for $\alpha = 3.98$ than for $\alpha = 1.99$. Such is the case as shown by the relatively small difference between the dash dot line from Lynn's work and our experimental points.

The experiments with the taller cylinder ($\alpha = 3.98$) thus bear out our earlier generalizations that the best agreement with theory occurs for the lowest inertial oscillation frequencies. In Lynn's notation we have found that for small values of $K = \frac{k\pi}{\alpha}$ differences are least between observed and predicted shifts of inertial eigenfrequencies during spin-up from rest.

Combined in figure 11 are the experimental points for the (2,1) mode from figure 7 and figure 9 for the two different cylinders $\alpha = 1.99$ (closed circles) and $\alpha = 3.98$ (triangles). For both sets of points in this figure the abscissa has been scaled with the frequency ratio $\frac{\Omega}{\omega}$ corresponding to $t \to \infty$ for direct comparison of the relative ω shifts in eigenfrequency. Presented in this way the experiments show a very weak dependence on $K = \frac{k\pi}{\alpha}$ of the shift in eigenfrequency with time since container switch-on. Lynn's work, as shown by the dash dot line which serves to present both aspect ratios when scaled in the manner just mentioned for the experiments, bears out this weak dependence. The discrepancy between the experimental points and the line is less for the tall cylinder ($\alpha = 3.98$) than for the short ($\alpha = 1.99$) one as noted earlier and reflects our comment that agreement with theory is better for lower frequency modes (smaller ω) relative to the rotation speed, Ω .

The generalizations given above with regard to agreement between experiment and Lynn's analytical work arose from experiments which were carried out at different amplitudes of perturbation, ε . The dependence on perturbation amplitude of our observed changes in inertial oscillation frequency with time since container switch-on was studied for the (2,1) mode. Shown in figure 12 is the observed change in frequency of the (2,1) mode ($\alpha = 3.98$) for each of several perturbation amplitudes in the range $\varepsilon = 3.18°$ to $\varepsilon = 6.46°$. Only that portion of the frequency change corresponding to the range 1.6 to 2.3 spin-up times from rest was studied in this detail for various perturbation amplitudes. No perturbation amplitude effects in the dependence of inertial oscillation frequency on time since container switch-on are apparent in figure 12. Since the perturbation amplitudes covered in this experiment span the range of perturbation amplitudes of the previous experiments we conclude that departures of our experimental results from Lynn's analytical results are probably not due to perturbation amplitude effects.

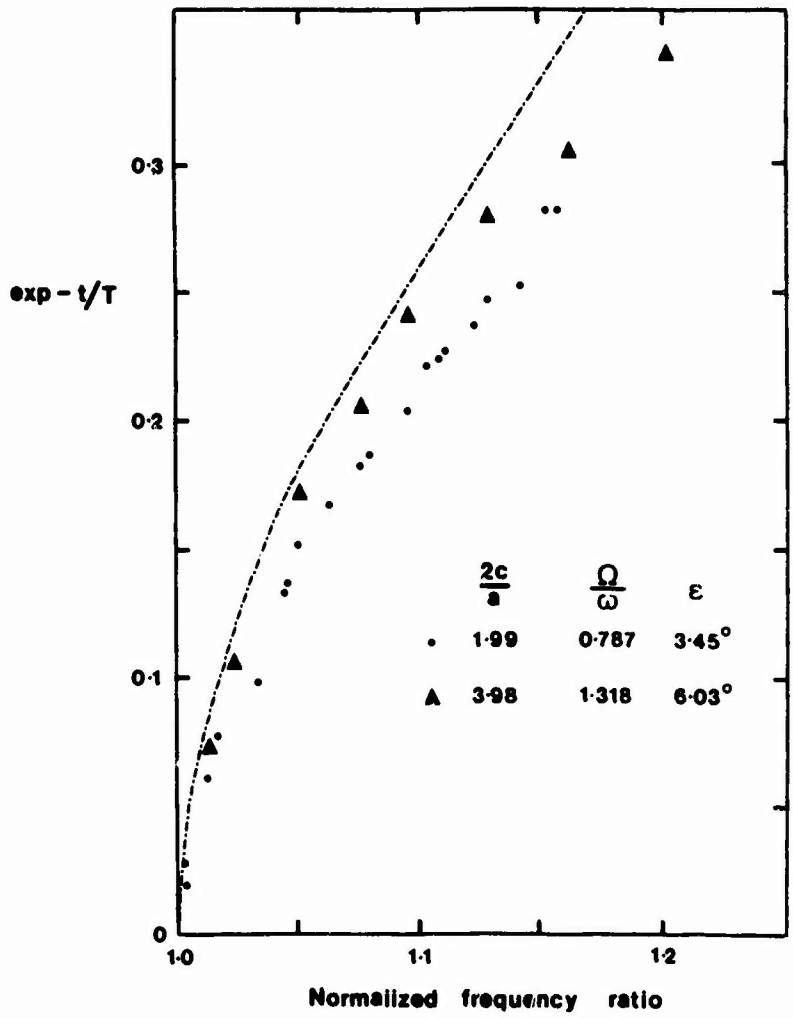

Figure 11. Dependence of inertial oscillation frequency (normalized in terms of frequency ratio $\frac{\Omega}{\omega}$ for $t \to \infty$) on time since switch-on for (2,1) mode in the cylinder α=1.99 (closed circles) and the cylinder α=3.98 (triangles). Curve is from Lynn (1973).

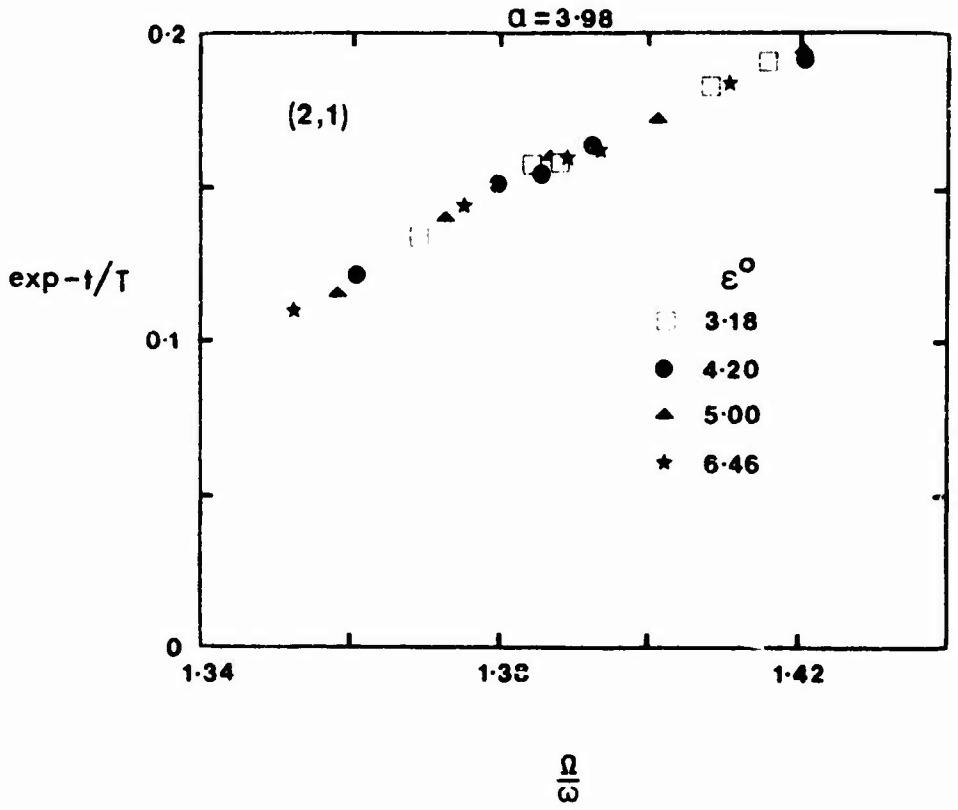

Figure 12. Dependence of inertial oscillation frequency on time since container switch-on for the (2,1) mode in the cylinder α=3.98 at various amplitudes ε of container perturbation.

5. Discussion

Inertial oscillations were identified in section 4 of this report by comparison of the frequency ratio $\frac{\Omega}{\omega}$ for maximum disturbance pressure response with the ratio predicted from inviscid linear theory. A small discrepancy, about 0.3% for the (2,1) mode (figure 2) and 0.4% for the (2,2) mode (figure 3), between experimental and theoretical values of $\frac{\Omega}{\omega}$ was left unexplained. On the basis of linear theory we would expect that the greatest response in disturbance pressure to occur at a value of $\frac{\Omega}{\omega}$ which is smaller than that calculated from inviscid theory by an amount proportional to $E^{\frac{1}{2}}$. In our experiments this amounts to less than 0.1% so that although observed maximum in disturbance pressure occurs at a smaller value of $\frac{\Omega}{\omega}$ than calculated from inviscid theory as expected, the actual shift is greater than expected.

In order to account for the few tenths of a percent in the difference between the calculated inviscid frequency ratio and the observed peak in disturbance pressure we refer back to relation (1). The only measurements required to obtain the predicted inviscid frequency ratio $\frac{\Omega}{\omega}$ for any mode is the aspect ratio of the cylinder, α . From relation (1) we find that the fractional error in $\frac{\Omega}{\omega}$ is related to the fractional error in α by a numerical factor which is 1.19 for the (2,1) mode and 1.66 for the (2,2) mode. Since the ratio of these factor is about the same as the ratio of the observed discrepancies 0.3% for the (2,1) mode and 0.4% for the (2,2) mode we suggest that a small uncertainty in the container aspect ratio accounts for these discrepancies.

The main purpose of our experiments has been to measure the eigenfrequencies of inertial oscillations while the fluid in a cylinder is spinning up from rest. The measured eigenfrequencies for the (2,1), (2,2) and (4,2) modes in the cylinder $\alpha = 1.99$ and the (2,1) and (4,2) modes in the cylinder $\alpha = 3.98$ compare favorably with those predicted by Lynn's analysis. We note, however, that all of our results were obtained after about one spin-up time from container switch-on because there was insufficient disturbance pressure before that point. Therefore we suggest that subsequent experiments be carried out at larger perturbation amplitudes, ε in order to increase the amplitude of disturbance pressures. No non-linear effects in the change in eigenfrequency with time since switch-on were observed with the amplitudes ε in the experiments described in this report. Hence we suggest extending the curves such as those shown in figure 7 to larger values of $e^{-t/T}$ by increasing ε .

An alternative method of increasing the disturbance pressure differences is to increase the perturbation frequency, ω . This is an attractive procedure since disturbance pressure is proportional to the perturbation frequency squared. Furthermore an increase in frequency ω requires an increase in rotation speed Ω which reduces the Ekman number. Although it is unlikely that any of the departures of our present

experimental results from theory are due to finite Ekman number effects since the largest Ekman numbers in our experiments are about 5×10^{-6}, even smaller Ekman numbers will make this statement more certain.

The departures from Lynn's results of our experimental results on the change in eigenfrequency with time since switch-on have been summarized in section 4. We have stated that best agreement between experiment and theory occurs for the lowest frequency oscillations or put another way those modes which have particle motions predominantly parallel to the axis of rotation. It is noteworthy that agreement between experiment and theory depends critically on how the experimental results are scaled. In our case we have followed Lynn's scaling since we are comparing our results with his analysis. It is interesting to note that although Lynn chooses $\chi = 1.0$ (section 3) rather than $\chi = 0.866$ as originally used by Wedemeyer in his model, this constant does not appear to enter into subsequent analysis. Hence we might consider the effect of presenting our observed times until peak disturbance pressure as $e^{-\chi t/T}$ with $\chi = 0.886$ instead of $\chi = 1.0$. This would have the effect of raising all the experimental points upward in figures 5, 7, 8, 9, 10, 11, 12 by such an amount that the points for the (2,1) mode in figure 7 would fall almost directly on the line in that figure. Furthermore all the points would then lie above the line rather than below so that the inertial oscillations would occur sooner in time than predicted or alternatively would show less shift in frequency than expected during the transient spin-up period. Such an interpretation would also be consistent with the experiments of Watkins and Hussey (1973) on spin-up from rest in a cylinder. They found that spin-up always occurred more rapidly than predicted by the Wedemeyer model. As mentioned in the introduction, however, the Ekman numbers in our experiments are sufficiently small that there should be only very minor departures from the spin-up predicted from Wedemeyer's analysis.

The choice of $\chi = 0.886$ has further ramifications in the interpretation of our experimental results. Better agreement with theory would then occur for a lower order (small number of nodal surfaces), mode (2,1) while agreement with a more complex mode (2,2) would be worse. This interpretation is appealing until we consider the much more complex (4,2) mode (figure 8) which would agree very closely with theory were $\chi = 0.886$ rather than 1.0. Hence a change in scaling of time, consistent with Lynn's analysis, appears to provide no net improvement in the interpretation of our experimental results.

The choice of value for χ is an important one which is apparently not determined in Lynn's analysis. The quantity $f = e^{-\chi t/T}$ giving the position of the velocity front over time since switch-on could be found experimentally. Hence the constant χ could be determined directly from experiments on spin-up from rest. We suggest therefore that experiments on impulsive spin-up should be undertaken to accomplish this. The apparatus used in the present experiments can be modified so that the container will be spun up within a fraction of a revolution in order to approximate impulsive spin-up from rest.

For the experiments described in this report the container achieved what was termed quasi-steady motion after about three revolutions. This means that some adjustment should be made for the non-impulsive nature of container rotation from rest. Even if we choose to ignore the first three revolutions in our measurement of time until maximum disturbance pressure is reached this leads to at most 4% error in time measurement. Although shorter times would have the effect of improving the agreement with theory in all the experiments, it is not obvious how to apply such a correction so that we present the results showing actual raw time measurements. Subsequent experiments involving the investigation of container acceleration will help to resolve this problem.

The term quasi-steady used above with regard to the rotation of the container refers to the fact that the mean rotation speed of the container, Ω, included in addition to the perturbation $\varepsilon\omega \cos\omega t$, a steady increase over the spin-up time of the fluid. This increase amounted to less than 3% over periods of several minutes. It is due to the feedback nature of the speed control (Appendix II) and comes about presumably because the moment of inertia of the rotating experiment is continually changing while the fluid spins up from rest. No corrections were applied for this slow steady acceleration of the container.

Acknowledgements

This work was carried out under U. S. Army Research Contract DAAD 05-74-Q-5383 while the author was associated with the Institute of Earth and Planetary Physics at the University of Alberta. Thanks are due to Nick Riebeek for technical assistance, Richard Adler for research assistance and Bill D'Amico for the calculations for the figures based on Lynn's (1973) analysis.

Appendix I

Calibrations

The frequency of oscillation, ω , was controlled by a signal generator. A precise measurement of this frequency was obtained by connecting the output of the signal generator to an electronic counter-timer. The frequency was constant to within ± .03% over the duration of several experimental runs.

The measurement of time from container switch-on until peak disturbance pressure was obtained from a distance measurement on a constant speed chart recorder. Speed of the chart paper was calibrated and checked by recording a sine wave of known frequency over a large number of cycles. The frequency of the sine wave was determined with the counter-timer as described above.

The rotation speed of the container was monitored continuously by displaying the output of a tachometer, connected directly to the rotating system, on the electronic counter-timer. The counter-timer showed the number of pulses from the tachometer in a fixed time (10 sec.) period. This number was converted to a rotation speed by a direct measurement of rotation speed over a larger interval with a stopwatch. Further details of the speed control are given in Appendix II.

Disturbance pressure measurements were made with a differential pressure transducer (NS LX3700D) of range ± 1.5 psi. The output of this transducer, amplified and filtered (Krohn-Hite, low frequency cut off 0.5 hertz, high frequency cut off 2.0 hertz), was displayed on a chart recorder (Techni-rite). In order to express the measured displacements on the chart recorder in terms of known pressure differences a calibration input was applied to the transducer. A beaker of water was oscillated vertically at the working frequency, ω , so that a known change in pressure was applied to the transducer via the hypodermic needle and tubing. Displacements of the support for the beaker were measured with a strain-guage and converted to millimeters of water pressure. (The tip of the hypodermic was sufficiently near the surface that dynamic corrections were negligible.) Shown in figure 13 are calibration data for two different probes used in our experiments. Probe 1 was used for the $\alpha = 1.99$ container while probe 2 was used for the $\alpha = 3.98$ container. The difference in response of the two probes is due mainly to the difference in position of the oil-water interface. Future experiments will use silicone oil throughout in order to avoid these surface tension effects.

The kinematic viscosity of the working fluid was measured using a Canon viscometer. Kinematic viscosity is found directly from a measurement of time for the fluid to move a known distance through precision capillary tube.

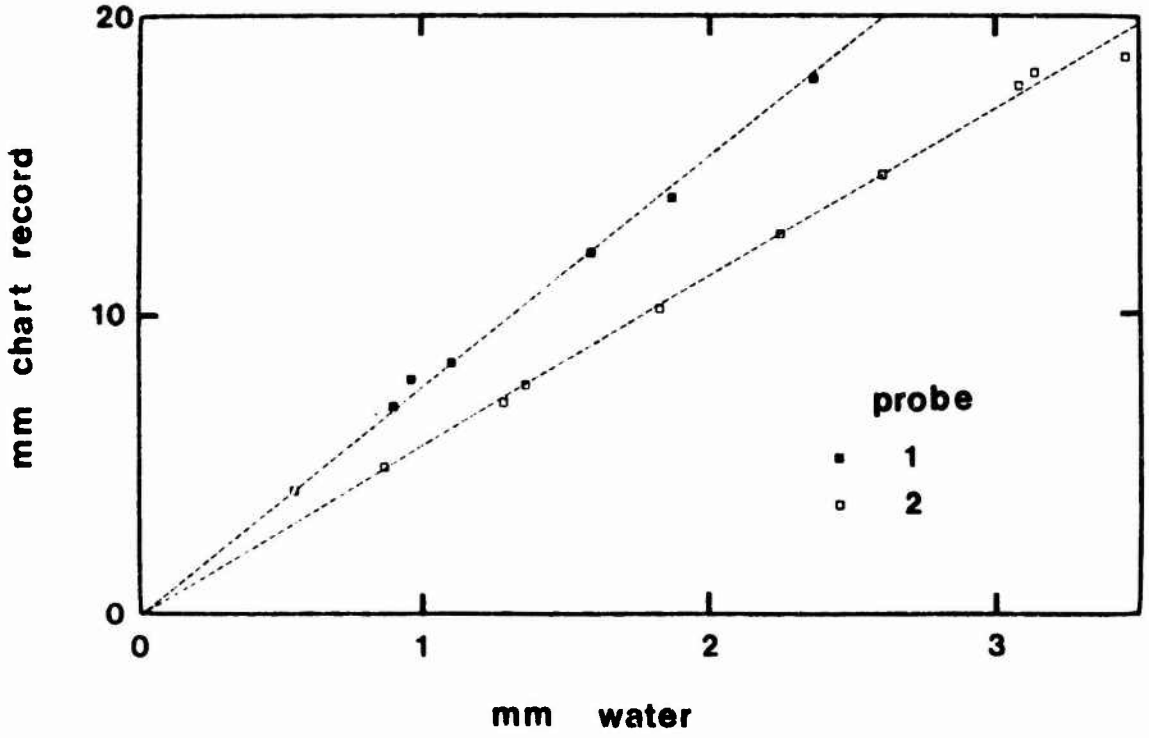

Figure 13. Amplitude calibration of Lx3700D pressure transducer. Ordinate gives measured displacement on chart record for a known change in pressure head given by the abscissa. Probe 1 was used for the cylinder α=1.99, probe 2 was used for cylinder α=3.98.

Appendix II

Motor speed control (Figure 14)

The operation of the motor control depends on the characteristic behaviour of an operational amplifier used in a closed loop configuration following the application of a voltage to its inputs. Specifically, such a device will drive whatever current is required through its load in order to generate sufficient feedback voltage, which is of opposite polarity to its input voltage, to drive its summing point (i.e. inverting input) back to the potential of its non-inverting input which is normally grounded. It is a condition of zero input voltage difference that such a device "desires" to maintain, and in the case of the RCA HC2000 device used here, this condition is closely approximated. The device has a maximum power dissipation of 60 watts if infinite heat sinking is provided.

In order to cause the amplifier to regulate the motor's speed, we must provide it with a feedback voltage which is proportional to the motor's speed of rotation and opposite in sign to the applied input voltage. This is accomplished here by an optical shaft encoder attached to the axis of the rotating system. The pulses produced by this device are processed through essentially a frequency to voltage conversion. This voltage is then used as the amplifier feedback.

We note here that even with a non-ideal amplifier (that is with non infinite gain), if the open-loop gain is high enough our system will be oscillatory, since the technometer feedback voltage will turn the amplifier off completely once the desired speed is attained and the system will exhibit a sawtooth shaped plot of motor speed against time. To smooth the systems response, the tachometer feedback is paralleled with a D.C. feedback path which reduces the gain from its open-loop value of three to four thousand to about twenty. An additional feedback control is available through a D.C. level adjustment provided in series with the tachometer's output. With this control it is possible to raise the gain, thus increasing the quality of the system's response, until just below the point where inertial and frictional dampings are no longer sufficient to prevent oscillation. This is the ideal operating point of the present system.

An RCA hybrid operational amplifier was chosen for its good approximation to a high power operational amplifier and reasonable cost. With adequate heat dissipation provided, it can deliver up to 7 amps with a bipolar output around 10 to 20 volts, depending on its power supply. In use here, it is provided with an input offset voltage nulling circuit and a frequency compensation network consisting of a 22 ohm resistor and 8 microhenry coil in parallel. It should be noted that

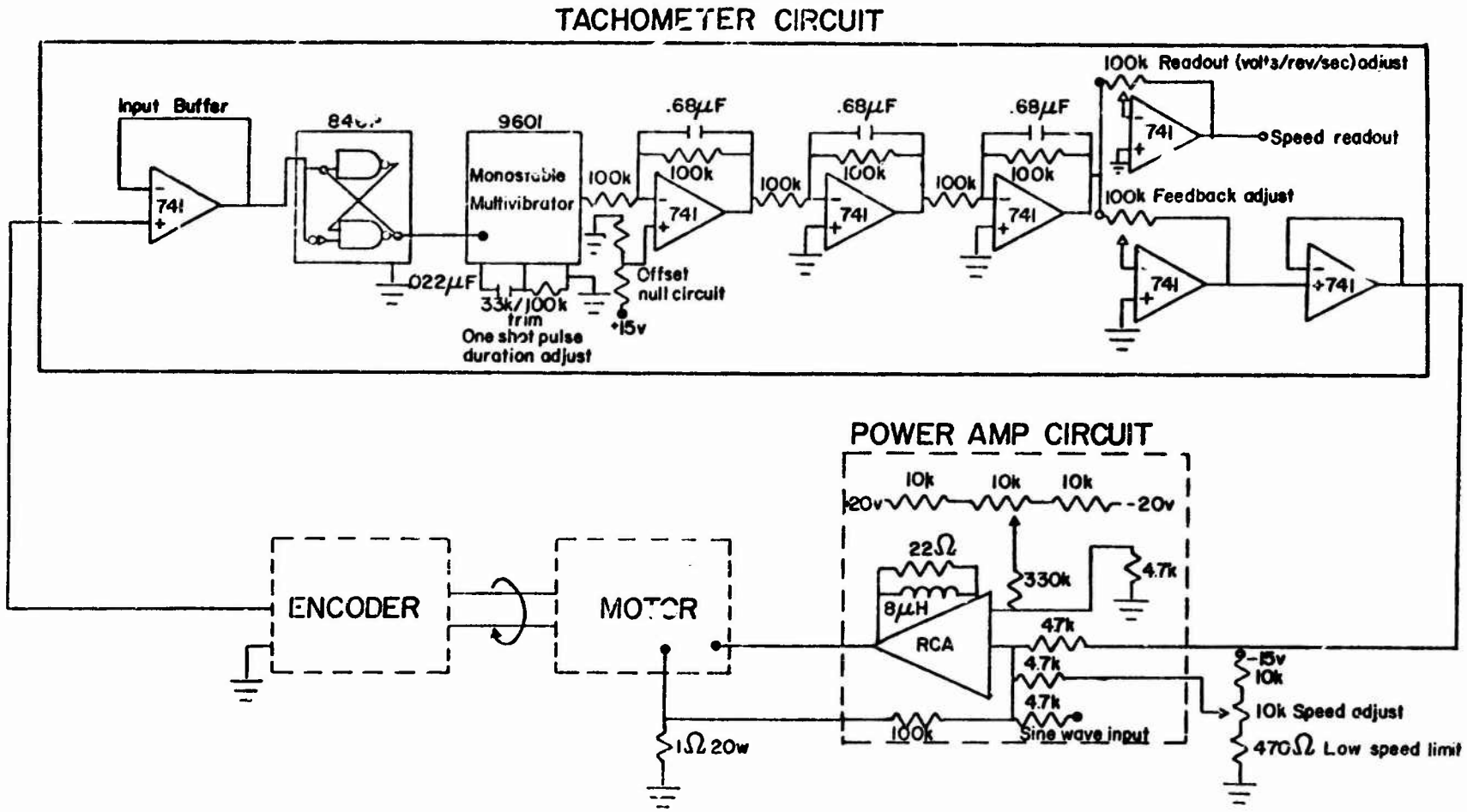

Figure 14. Schematic for motor speed control.

these devices must dissipate considerable power when the amplifier's output is made to slew at even a few hertz.

A Theta optical shaft encoder was chosen as a rotation sensor for its large number of read events per revolution. It produces 250 quasi-sinusoidal pulses per revolution of its input shaft. The tachometer electronics consist of a Fairchild model 9601 integrated circuit monostable multivibrator which produces constant amplitude and constant (adjustable) duration pulses from the encoder output which is squared by crosscoupled nand gates in an MC846P integrated circuit. This pulse train has to have a duty cycle of less than 80% at the highest rotation speed used, or the pulses cease to be of the preset duration. Thus when the system is rotating slowly, the duty cycle is around 5 to 10 percent. Integration is required to arrive at a smooth D.C. output from such an input. To ensure this, a series of three active integration stages was employed. The first includes a circuit for nulling the output voltage offset of the 9601. Before this integration, the one shot pulses are fed into a pulse frequency counter, which displays the turntable rotation speed (times 250) for the operator. The integrated output is split into two parts, each of which passes through a variable gain amplifier. One is adjusted to give an output voltage of approximately one volt per rev/sec of the system and is displayed on a digital voltmeter to provide a measure of the small rapid pace speed changes of the system. These cannot be seen on the pulse counter speed readout, because it has an integration time (while it counts up pulses) of the order of one second. The second part of the tachometer signal is fed through a similar adjustable gain amplifier which serves as the feedback adjustment previously mentioned. Its output is then buffered and sent to the power amplifier.

References

Aldridge, K. D., 1975, Inertial waves and the Earth's outer core. Geophys. J., to appear in July, 1975.

Aldridge, K. D. and Toomre, A., 1969, Axisymmetric inertial oscillations of a fluid in a rotating spherical container, J. Fluid Mech., 37, 307.

Aldridge, K. D., 1972, Axisymmetric inertial oscillations of a fluid in a rotating spherical shell, Mathematika 19, 163.

Bjerknes, V., J. Bjerknes, H. Solberg and T. Bergeron, 1933, Physikalische Hydrodynamik, Berlin, J. Springer.

Fultz, D., 1959, A note on overstability and the elastoid-inertia oscillations of Kelvin, Solberg and Bjerknes, J. Meteorol. 16, 199.

Greenspan, H. P., 1968, The theory of rotating fluids, Cambridge University Press.

Greenspan, H. P. and L. N. Howard, 1963, On the time-dependent motion of a rotating fluid 17, 385.

Kelvin, Lord, 1880, Vibration of a columnar vortex, Phil. Mag. 10, 155.

Lynn, Y. M., 1973, Free oscillations of a liquid during spin-up, Ballistics Research Laboratories Report No. 1663.

Watkins, W. B. and R. G. Hussey, 1973, Spin-up from rest: Limitations of the Wedemeyer model, Phys. Fluids 16, 1530.

Wedemeyer, E. H., 1964, The unsteady flow within a spinning cylinder, J. Fluid Mech. 20, 383.

Weidman, P., 1973, On the spin-up and spin down of a rotating fluid, To be published in J. Fluid Mech.